The 2009 IEEE/RSJ International Conference on
Intelligent Robots and Systems
October 11-15, 2009 St. Louis, USA

Metal-filled Carbon Nanotubes for Nanofluidic Systems: Modes of Melting and Evaporation

Lixin Dong, Xinyong Tao, Li Zhang, Xiaobin Zhang, and Bradley J. Nelson

Abstract— **Modes of melting and evaporation of metal at attogram level from individual carbon nanotubes (CNTs) are investigated experimentally using nanorobotic manipulation inside a transmission electron microscope. We compared the melting and evaporation induced by electric current, Joule heating, charge, and ionization. Experiments show that the most effective method is by positively ionizing the encapsulated metal, therefore, an electrostatic field can be used to guide the flow. Applications and potential applications of mass transport and deposition in nanofluidic systems have been presented including self-welding, actuation, and storage.**

Index Terms—**Carbon nanotube, transmission electron microscope, nanofluidics, nanorobotic manipulation**

I. Introduction

CONTROLLED melting and flowing of mass within and between nanochannels is of great interest both fundamentally and from an application perspective [1-9]. We report an experimental investigation into attogram copper evaporation from individual carbon nanotubes (CNTs), which is motivated by the need to understand the mechanism of this phenomenon. Copper has played a significant role in the history of civilization. In modern semiconductor industry, copper is increasingly replacing aluminum because of its superior electrical conductivity. Growing interest in using it as electrodes and functional elements for the next generation of integrated circuits has been stimulated by the discovery of CNTs, nanowires, and other building blocks, and enabled by bottom-up nanotechnologies such as self-assembly [10], robotic assembly [11, 12], and welding [6, 13]. With the possibility of delivering attogram copper from conduits [6, 7], copper-filled CNTs [14] are an ideal combination for self-welding of self-assembled nanotubes [10] onto electrodes, among other potential nanofluidic applications [9, 15-17].

Previous experimental investigations of controlled melting and flowing of single crystalline copper from individual CNTs [6, 7] have shown that very low current induces melting and drives the flow, which is much more efficient than irradiation-based techniques involving high energy electron beams [18-21], focused-ion beams (FIB) [22], or lasers [16]. Furthermore, conservation of the material is facilitated by its encapsulation as opposed to conveying mass on the external surface of nanotubes [23]. Because both the rate and direction of mass transport depend on the external electrical drive, precise control and delivery of minute amounts of material is possible. However, due to the coupling of the electronic and thermal effects, the mechanisms have not been well understood.

II. Modes of Melting and Evaporation

To understand the mechanisms induced by various physical effects, experimental investigations have been done using the setup shown in Fig. 1, where two Cu-filled CNTs supported on a common sample holder and a probe provide four different experimental modes (Table I): (1) The upper section of the left nanotube, $CNT_{1,A}$, has electric current passing through and accordingly Joule heating will occur. (2) The lower section of the left nanotube, $CNT_{1,B}$, has no current and will experience only thermal transport. In (3) and (4), the right tube, CNT_2, has no electric current but can be either

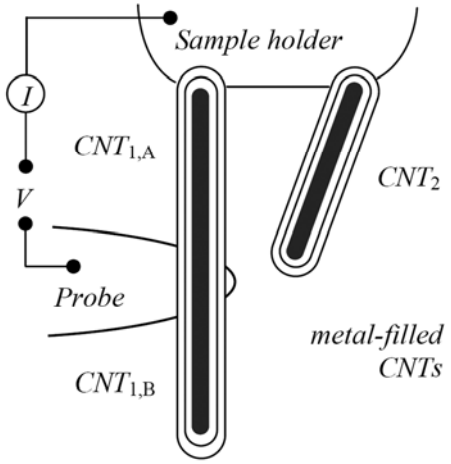

Fig. 1. Experimental setup. Two Cu-filled CNTs supported on a sample holder and a probe provide three different cases to investigate, $CNT_{1,A}$, $CNT_{1,B}$, and CNT_2, subjected to electric current, thermal transport, and charges, respectively.

Manuscript received March 1, 2009. This work is conducted with financial support from the ETH-Zurich, the Chinese National Science Foundation (No. 50571087); the Hi-tech Research and Development Program of China (863) (2002 AA334020), and the Natural Sciences Fund of Zhejiang Province (Y404274).

L. X. Dong, L. Zhang, and B. J. Nelson are with the Institute of Robotics and Intelligent Systems, ETH Zurich, 8092 Zurich, Switzerland (phone: +41-44-632-2539; fax: +41-44-632-1078; e-mail: ldong@ethz.ch). L.X. Dong is currently with the Department of Electrical & Computer Engineering, Michigan State University, East Lansing, MI 48824-1226, U.S.A.

X.Y. Tao is with the College of Chemical Engineering and Materials Science, Zhejiang University of Technology, Hangzhou 310032, China, and was with the Department of Materials Science and Engineering, Zhejiang University, Hangzhou 310027, China.

X.B. Zhang is with Department of Materials Science and Engineering, Zhejiang University, Hangzhou 310027, China.

TABLE I MODES OF MELTING AND EVAPORATION

CNT	Current	Heat	Ionization	Charge
$CNT_{1,A}$	Yes	Yes		
$CNT_{1,B}$	No	Yes		
CNT_2			Probe -	Probe +

negatively charged or positively ionized. Thermal transport also occurs from the common sample holder, but not as directly as $CNT_{1,B}$ due to CNTs superior heat conduction ability (Thermal conductivity: 3320 W/m·K; c.f. Ag: 429 W/m·K, Cu: 386 W/m·K, Au: 318 W/m·K) [24].

The samples we use are Cu-filled CNTs. As described elsewhere, the Cu-tipped CNT samples are synthesized using an alkali doped Cu catalyst by a thermal chemical vapor deposition (CVD) method [14]. The CNTs are up to 5 μm long with outer diameters in a range of 40–80 nm. The single crystalline Cu nanoneedles are encapsulated in graphite walls approximately 4 to 6 nm thick at the tips of CNTs. The graphite layers are not parallel to the tube axis.

Our experiments were performed in a Philips CM30 transmission electron microscope (TEM) equipped with a scanning tunneling microscope (STM) built in a TEM holder (Nanofactory Instruments AB, ST-1000) serving as a manipulator [2, 6, 25]. The material consisting of a CNT bundle is attached to a 0.35 mm thick Au wire using silver paint, and the wire is held in the sample holder (Fig. 1). An etched 10 μm thick tungsten wire with a tip radius of approximately 100 nm (Picoprobe, T-4-10-1mm) is used as the probe. The probe can be positioned in a millimeter-scale workspace with sub-nanometer resolution with the STM unit actuated by a three-degree-of-freedom piezo-tube, making it possible to select a specific CNT and pick it up. Physical contact can be made between the probe and the tip of a nanotube or between two nanotubes. Applying a voltage between the probe and the sample holder establishes an electrical circuit through a CNT and injects thermal energy into the system via Joule heating. By increasing the applied voltage, the local temperature can be increased past the melting point of the material encapsulated in a tube. The process is recorded by TEM images, a multimeter, and a nA meter.

Figure 2 includes a series of TEM images recording the evaporation of Cu driven by current and Joule heating inside two single CNTs when the probe is positively biased (7 V). It can be seen that the length of the copper core inside the CNT on the left side (both $CNT_{1,A}$ and $CNT_{1,B}$) decreases continuously. Figure 3 is a series of TEM images recording the transport of Cu inside two single CNTs when the probe is negatively biased (-3.5 V). It can be seen that the length of the copper core inside the CNT on the left side ($CNT_{1,B}$) also decreases continuously. Because the copper core is not between the electrodes, the polarity of the electrodes does not matter, copper will transport towards one of them.

Surprisingly, it can be seen from Fig. 3 that the length of the copper core inside the CNT on the right side (CNT_2) also decreases continuously until almost all copper disappears. A closer inspection of the insets of Fig. 2 reveals the same phenomena occurred when the probe is positively biased. This implies the possibility that charge induced transport is more significant than current-induced Joule heating and thermal transport. The obvious difference of the evaporation rate for Cu inside CNT_2 suggests that as the Cu is positively ionized (Fig. 3), the repulsive forces between Cu ions are

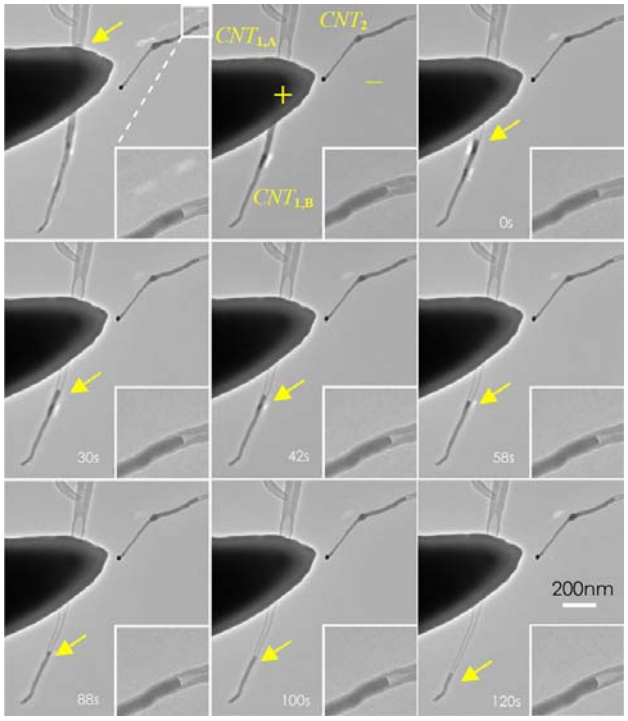

Fig. 2. Electric current and Joule heating driven Cu evaporation. A series of TEM images recorded the transport of Cu inside two single CNTs when the probe is positively biased (7V). It can be seen that the length of the copper core inside the CNT on the left side continuously decreases.

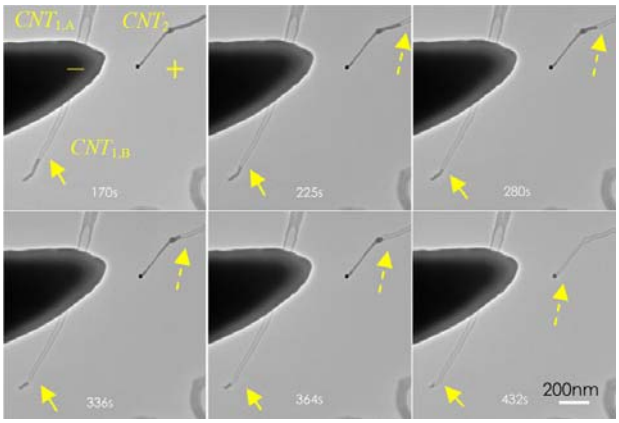

Fig. 3. Thermal transport and positive charges induced Cu evaporation. A series of TEM images recorded the transport of Cu inside two single CNTs when the probe is negatively biased (-3.5V). It can be seen that the length of the copper core inside the CNT on the left side also continuously decreases.

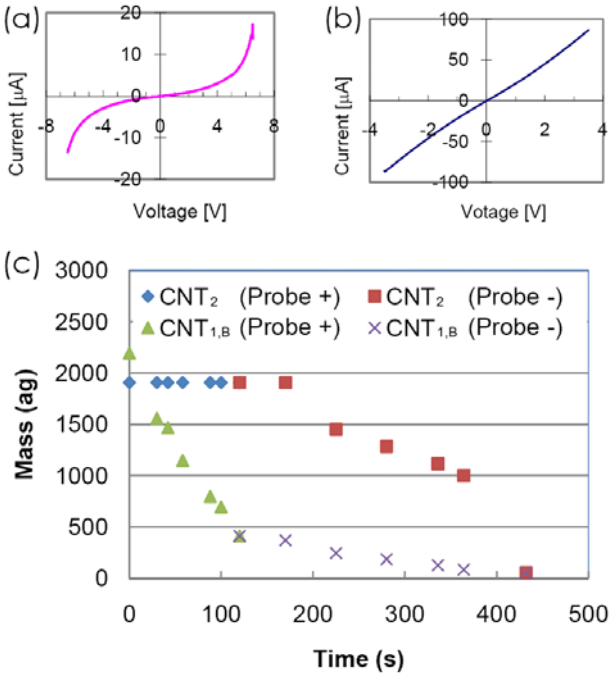

Fig. 4. (a) and (b) are I-V curves before the threshold on positive and negative biases is reached. It can be seen by comparing (a) and (b) that conductance improved after copper transport (the minimum resistance changed from (a) 377 kΩ to (b) 40 kΩ). (c) Mass evaporation rate.

larger than negatively charged case (Fig. 2).

Figure 4(a) and (b) are I-V curves before the positive and negative threshold biases are reached. It can be seen by comparing Fig. 4(a) and (b) that the conductance improved after the copper was transported (the minimum resistance changed from Fig. 4(a) 377 kΩ to Fig. 4(b) 40 kΩ). This suggests copper deposited on the probe in the case of Fig. 4(a) changed the contact from a Schottky-type to Ohmic. The decrease of resistance from 477 kΩ (-6.5 V) to 377 kΩ (6.5 V) in the case of Fig. 4(a) indicates the transport/deposition on the probe occurred during the bias sweeps from -6.5 V to 6.5 V.

Figure 4(c) indicates the estimated mass evaporation rate according to the apparent geometries shown in Figs. 1 and 2 and the density of copper (8.92 g/cm^3). Using linear fitting, the average mass evaporation rate has been found to be 14.3 ag/s and 1.2 ag/s for $CNT_{1,B}$ as the probe is positively (Fig. 2) and negatively (Fig. 3) biased, respectively. The difference (approximately 12 times) between the rates of $CNT_{1,B}$ is due to the competition between electrostatic forces and Joule heating induced evaporation. The latter is mainly caused by the different absolute values of the bias V (7 V and -3.5 V) and the resistance R (377 kΩ to 40 kΩ). Considering that thermal power scales with V^2/R, the bias differences translate into a factor of 2.4, but the evaporation rate as the probe is negatively biased should be larger. This is contrary to the experimental observation. Hence, it can be concluded that electrostatic forces dominate evaporation. The growing

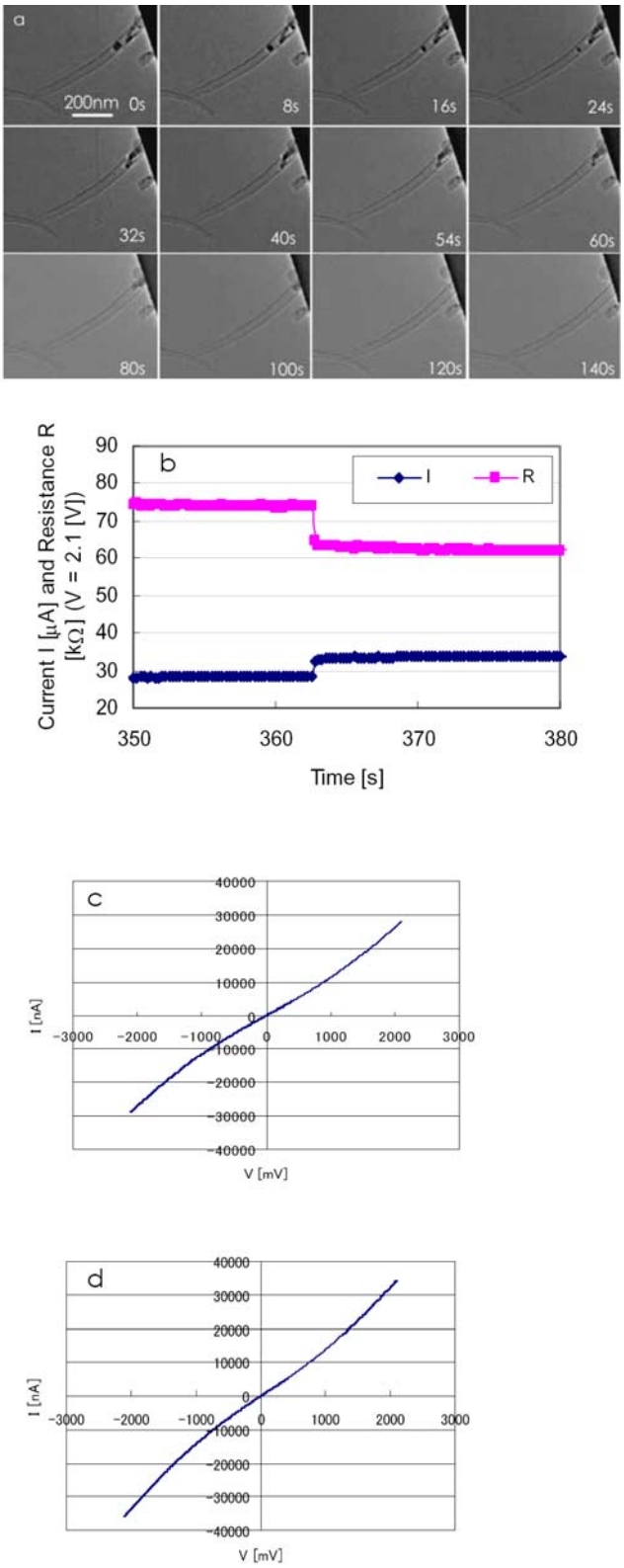

Fig. 5 Intra-nanotube mass (Cu) transport. (a) Further flowing the received copper (bias 2.1V) from the cap-opened CNT to the electrode (a Pt-coated AFM cantilever). (b) Contact resistance improved when copper diffused onto the AFM cantilever (Cantilever as anode). (c-d) I-V curves show the contact resistance improved when copper diffused onto the cantilever: (c) before melting and (d) after melting.

distance from the heated section also has contribution but less due to the excellent thermal conductivity of CNTs.

Similarly, using linear fitting, the average mass evaporation rate has been found to be 0.1 ag/s and 6.1 ag/s for CNT_2 as the probe is positively (Fig. 2) and negatively biased (Fig. 3), respectively. This suggests that when Cu is ionized, the repulsive interaction between Cu^+ is much larger than electron charges.

III. Current-driven Melting and Evaporation for Self-sorldering

Figure 5 shows the intra-nanotube Cu transport. Figure 5(a) reveals flowing of the copper (bias 2.1 V) from a cap-opened CNT to the electrode (a Pt-coated AFM cantilever). It can be seen from Fig. 5(b) that the contact resistance improved when copper diffused onto the AFM cantilever (as anode). Figure 5(c-d) are I-V curves shown the contact resistance improved when copper diffused onto the cantilever before melting (Figure 5(c)) and after melting

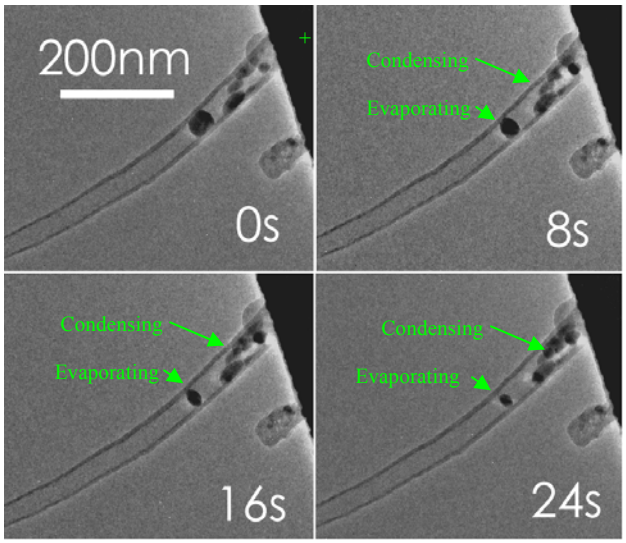

Fig.6 Evaporation and condensation

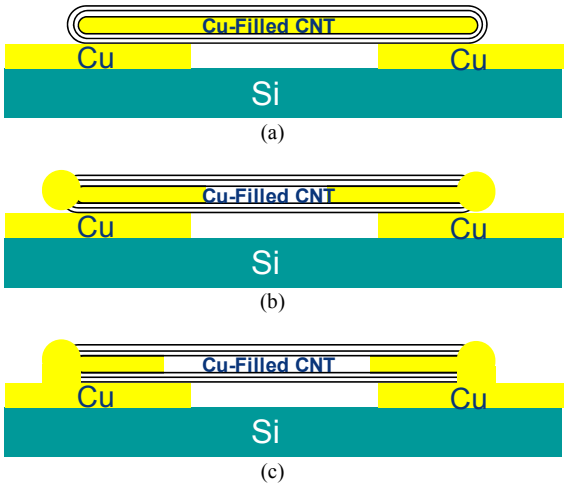

Fig. 7 Self-soldering of carbon nanotubes onto nanelectrodes. (a) self-assembled copper-filled nanotube. (b) AC-current driven flowing of copper from the nanotube. (c) Self-soldered nanotube.

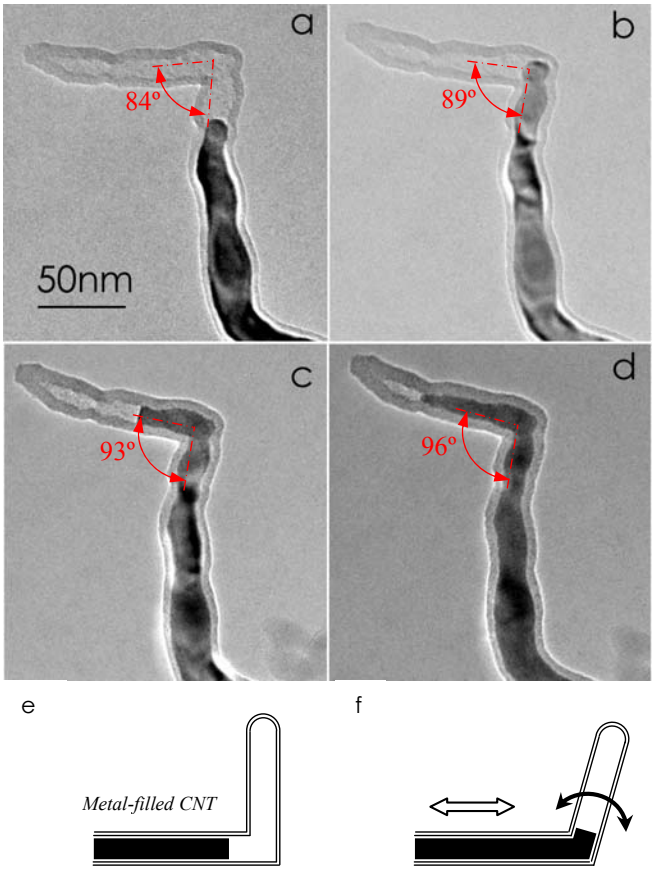

Fig. 8 Electron-beam induced flowing straighten a kinked Sn-filled CNT like what happens in a soft water pipe. After exposing under the e-beam with higher intensity for 1 min., images (a) to (d) were taken at ordinary intensity. This flow-induced deformation can find potential applications as a switch or clamper (e-f).

(Figure 5(d)). Figure 6 shows the details of the evaporation and condensation of the copper. The volume of the copper is decreasing at the site indicated with "evaporation" and increasing at the site close to the probe (anode); suggesting the condensation of the material. It should be noted that the temperature close to the probe (heat sink) is lower.

Current-driven flowing of copper from nanotubes has been presented for nanorobotic spot welding [6]. With a combination of self-assembly, self-soldering of nanotubes onto nanoelectrodes can be potentially enabled. As schematically shown in Fig. 7, a self-assembled nanotube (Fig. 7(a)) can be heated by an AC-current passing through it, then the encapsulated materials can be flowed out (Fig. 7(b)) based on the mechanism revealed above and solder the nanotube onto the electrodes (Fig. 7 (c)).

IV. Charge-induced Flowing for Actuation

Due to the fluidic pressure on the side walls of CNT, metal flowing in a kink junction of CNTs can induce the deformation of the junction. Figure 8 shows experimental investigation of this phenomenon. To keep the nanotube free-standing, electron-beam induced flowing is applied in stead of current driven one. It can be seen from Fig. 8, a

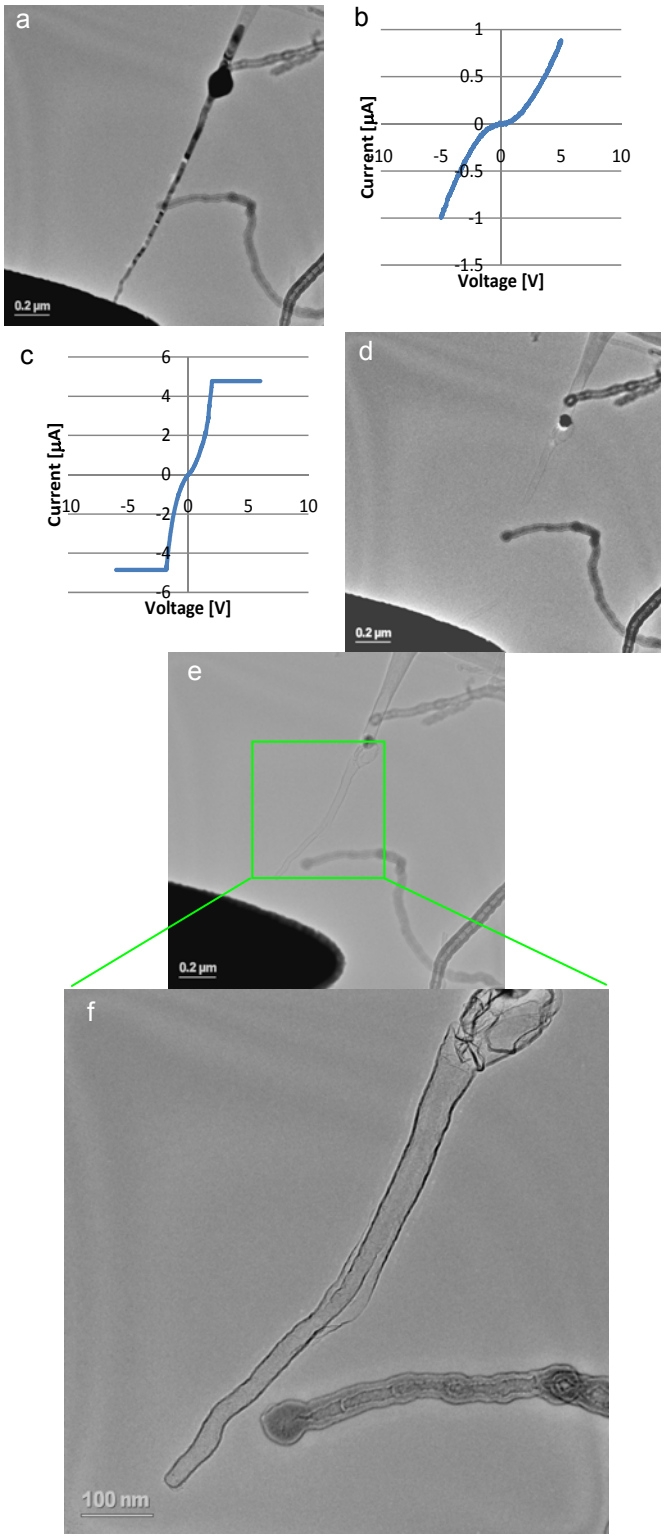

Fig. 9 Mode shifting from current-induced melting and evaporation to ionization-induced explosive evaporation. (a) and (b) show a Cu-filled CNT contacted with a probe (bias voltage: 5V) and an I-V curve of it. The maximum current is approximately 1.0 μA (993.8 nA); giving a resistance of 5 MΩ. When the bias was increased from 5 V to 6 V within 0.5 s, the current saturated (c) and the nanotube was broken (d). The record from a multimeter connected in the circuit shows the maximum current is 26.1 μA (Resistance: 229.9 kΩ). Then, the bias was removed and the tube was reconnected ((e) and (f)).

Sn-filled CNT is exposed to the higher intensity e-beam (CM30 TEM, 30kV) for 1 min intervals. After each exposure, an image (Fig. 8(a) to (d)) was taken at ordinary intensity. In the whole process, a 12-degree deflection of the junction is observed, which induced a c.a. 35 nm displacement at the free-standing tip of the nanotube (the arm length of the horizontal tube is c.a. 110 nm). With its ultra-compact sizes, such nanotube-based fluidic junctions can be potentially used as actuators for creating nanorelays, grippers, or manipulators. Further investigations are undergoing for improving the controllability using current-driven mechanism. This flow-induced deformation can find potential applications as a switch or clamper (Fig. 8 (e, f)).

V. Ionization-induced Draining for Mass Storage

Experiments show that the speed to increase the bias voltage influences the mode of melting and evaporation. Melting or evaporation will improve the conductivity, which means once flowing starts, current will increase under the same bias due to the improvement of the contact conductivity. If the bias increased with a too big step, the current may overpass the capacity of the nanotube; causing a sudden broken of the tube and an explosive evaporation of the copper. Ionization of the copper makes the evaporation continued after the tube was broken, i.e., after the current disappeared. Figure 9 (a) and (b) show a Cu-filled CNT contacted with a probe (bias voltage: 5V) and an I-V curve of it. The maximum current is approximately 1.0 μA (993.8 nA); giving a resistance of 5 MΩ. When the bias was increased from 5 V to 6 V within 0.5 s, the current saturated (Fig. 9(c)) and the nanotube was broken (Fig. 9(d)). The record from a multimeter connected in the circuit shows the maximum

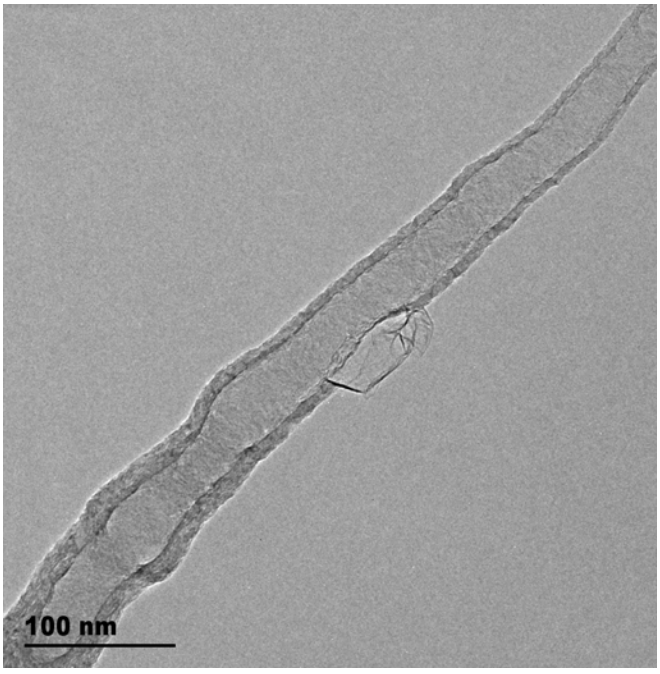

Fig. 10 Large hollow space left after draining the encapsulated copper.

current is 26.1 μA (Resistance: 229.9 kΩ). Then, the bias was removed and the tube was reconnected (Fig. 9(e) and (f)). No residual copper was found at the tip of the nanotube, which suggests deposited copper between the tip and the probe originally contributed to the improvement of the conductivity has also been evaporated due to ionization.

Ionization can induce multiple Cu-needles in neighboring tube tips disappear in one batch and leave large hollow space inside the tubes (Fig. 10). Because this process can be done in a non-contact fashion by either heating or ionization, and the ratio between the inner diameters to the wall thickness can be larger than non-filled nanotubes, they can potentially serve as better containers for hydrogen storage.

VI. Summary

In summary, we have reported an experimental investigation into attogram melting and evaporation of metal from individual CNTs using nanorobotic manipulation inside a transmission electron microscope. We compared the melting and evaporation induced by four modes induced by electric current, Joule heating, charges, and ionization. The experimental setup allowed the decoupling of the modes from each other. Experiments have shown that the most effective way for evaporation is by positively ionizing the encapsulated copper, which indicate that the repulsive electrostatic energy between copper ions dominate thermal energy, therefore, an electrostatic field can be used to guide the flow. The proposed CNT boilers can serve as sources for mass transport and deposition in nanofluidic systems using electrostatic fields to guide the flow. Applications and potential applications of mass transport and deposition in nanofluidic systems have been presented including self-welding, actuation, and storage.

Acknowledgment

The authors would like to thank the support from Electron Microscopy ETH Zurich (EMEZ).

References

[1] Y. H. Gao and Y. Bando, "Carbon nanothermometer containing gallium - gallium's macroscopic properties are retained on a miniature scale in this nanodevice," *Nature,* vol. 415, p. 599, Feb 2002.

[2] K. Svensson, H. Olin, and E. Olsson, "Nanopipettes for metal transport," *Physical Review Letters,* vol. 93, art. no. 145901, Oct 2004.

[3] A. K. Schaper, F. Phillipp, and H. Q. Hou, "Melting behavior of copper nanocrystals encapsulated in onion-like carbon cages," *Journal of Materials Research,* vol. 20, pp. 1844-1850, Jul 2005.

[4] L. Sun, F. Banhart, A. V. Krasheninnikov, J. A. Rodriguez-Manzo, M. Terrones, and P. M. Ajayan, "Carbon nanotubes as high-pressure cylinders and nanoextruders," *Science,* vol. 312, pp. 1199-1202, May 2006.

[5] M. Majumder, N. Chopra, R. Andrews, and B. J. Hinds, "Nanoscale hydrodynamics - enhanced flow in carbon nanotubes," *Nature,* vol. 438, pp. 44-44, Nov 2005.

[6] L. X. Dong, X. Y. Tao, L. Zhang, X. B. Zhang, and B. J. Nelson, "Nanorobotic spot welding: Controlled metal deposition with attogram precision from copper-filled carbon nanotubes," *Nano Letters,* vol. 7, pp. 58-63, Jan. 2007.

[7] D. Golberg, P. Costa, M. Mitome, S. Hampel, D. Haase, C. Mueller, A. Leonhardt, and Y. Bando, "Copper-filled carbon nanotubes: Rheostatlike behavior and femtogram copper mass transport," *Advanced Materials,* vol. 19, pp. 1937-1942, Aug 2007.

[8] P. M. F. J. Costa, D. Golberg, M. Mitome, S. Hampel, A. Leonhardt, B. Buchner, and Y. Bando, "Stepwise current-driven release of attogram quantities of copper iodide encapsulated in carbon nanotubes," *Nano Letters,* vol. 8, pp. 3120-3125, Oct 2008.

[9] L. X. Dong, X. Y. Tao, M. Hamdi, L. Zhang, X. B. Zhang, A. Ferreira, and B. J. Nelson, "Nanotube fluidic junctions: Inter-nanotube attogram mass transport through walls," *Nano Letters,* vol. 9, pp. 210-214, Jan 2009.

[10] A. Subramanian, L. X. Dong, J. Tharian, U. Sennhauser, and B. J. Nelson, "Batch fabrication of carbon nanotube bearings," *Nanotechnology,* vol. 18, art. no. 075703, Feb 2007.

[11] L. X. Dong, A. Subramanian, and B. J. Nelson, "Carbon nanotubes for nanorobotics," *Nano Today,* vol. 2, pp. 12-21, Dec 2007.

[12] L. X. Dong, F. Arai, and T. Fukuda, "Nanoassembly of carbon nanotubes through mechanochemical nanorobotic manipulations," *Japanese Journal of Applied Physics Part 1-Regular Papers Short Notes & Review Papers,* vol. 42, pp. 295-298, Jan. 2003.

[13] H. Hirayama, Y. Kawamoto, Y. Ohshima, and K. Takayanagi, "Nanospot welding of carbon nanotubes," *Applied Physics Letters,* vol. 79, pp. 1169-1171, Aug 2001.

[14] X. Y. Tao, X. B. Zhang, J. P. Cheng, Z. Q. Luo, S. M. Zhou, and F. Liu, "Thermal cvd synthesis of carbon nanotubes filled with single-crystalline Cu nanoneedles at tips," *Diamond and Related Materials,* vol. 15, pp. 1271-1275, Sep 2006.

[15] S. Supple and N. Quirke, "Rapid imbibition of fluids in carbon nanotubes," *Physical Review Letters,* vol. 90, art. no. 214501, May 2003.

[16] P. Kral and D. Tomanek, "Laser-driven atomic pump," *Physical Review Letters,* vol. 82, pp. 5373-5376, 1999.

[17] M. Whitby and N. Quirke, "Fluid flow in carbon nanotubes and nanopipes," *Nature Nanotechnology,* vol. 2, pp. 87-94, Feb 2007.

[18] L. X. Dong, F. Arai, and T. Fukuda, "Electron-beam-induced deposition with carbon nanotube emitters," *Applied Physics Letters,* vol. 81, pp. 1919-1921, Sept. 2002.

[19] T. Yokota, M. Murayama, and J. M. Howe, "In situ transmission-electron-microscopy investigation of melting in submicron al-Si alloy particles under electron-beam irradiation," *Physical Review Letters,* vol. 91, art. no. 265504, Dec 2003.

[20] S. Y. Xu, M. L. Tian, J. G. Wang, H. Xu, J. M. Redwing, and M. H. W. Chan, "Nanometer-scale modification and welding of silicon and metallic nanowires with a high-intensity electron beam," *Small,* vol. 1, pp. 1221-1229, Dec 2005.

[21] G. Q. Xie, M. H. Song, K. Furuya, D. V. Louzguine, and A. Inoue, "Compound nanostructures formed by metal nanoparticles dispersed on nanodendrites grown on insulator substrates," *Applied Physics Letters,* vol. 88, p. 263120, Jun 2006.

[22] R. Kometani, K. Kanda, Y. Haruyama, T. Kaito, and S. Matsui, "Evaluation of field electron emitter fabricated using focused-ion-beam chemical vapor deposition," *Japanese Journal of Applied Physics Part 2-Letters & Express Letters,* vol. 45, pp. L711-L713, Jul 2006.

[23] B. C. Regan, S. Aloni, R. O. Ritchie, U. Dahmen, and A. Zettl, "Carbon nanotubes as nanoscale mass conveyors," *Nature,* vol. 428, pp. 924-927, Apr 2004.

[24] P. G. Collins and P. Avouris, "Nanotubes for electronics," *Scientific American,* vol. 283, pp. 62-69, Dec 2000.

[25] L. X. Dong, K. Y. Shou, D. R. Frutiger, A. Subramanian, L. Zhang, B. J. Nelson, X. Y. Tao, and X. B. Zhang, "Engineering multiwalled carbon nanotubes inside a transmission electron microscope using nanorobotic manipulation," *IEEE Transactions on Nanotechnology,* vol. 7, pp. 508-517, Jul 2008.